

Rapid hydrofracture of icy moon shells: insights from glaciology

Robert Law^{1,2}

¹University of Bergen, ²Bjerknes Centre for Climate Research

robert.law@uib.no

Manuscript will be submitted to JGR Planets.

Europa's surface features many regions of complex topography termed 'chaos terrains'. One set of hypotheses for chaos terrain formation require upward migration of liquid water from perched water bodies formed by convection and tidal heating within the icy shell. However, consideration of the behaviour of terrestrial ice sheets suggests the rapid downwards, not upwards, movement of water from perched water bodies, initiated through hydrofracture and without a propagation limit provided there is a sufficient volume of water to fill the resulting vertical fracture. I suggest that drainage of perched water bodies to the subsurface ocean through hydrofracture is a likely phenomenon at Europa and other icy moons. This may at first appear to rule out perched water bodies in the formation of chaos areas, but the violence of such drainage events and loss of mechanical support could lead to the collapse of the surface shell and a temporary surface-ocean connection. Alternatively, hydrofracture provides a mechanism for entire ice-shell fracture if a surface impact melts enough near-surface ice.

Introduction

The presence of liquid water in icy moons beyond the asteroid belt was hypothesised by Lewis (1971) and supported by surface images and magnetic field readings from the Voyager, Galileo, Cassini satellite missions (e.g. [Squyres et al., 1983](#); [Carr et al., 1998](#); [Khurana et al., 1998](#); [Porco et al., 2006](#); [Lorenz et al., 2008](#); [Hendrix et al., 2019](#)). The presence of liquid water in these moons offers the tantalising possibility of extraterrestrial biology, which focussed research into whether the other basic requirements, chemical energy to drive metabolism and organic matter, may also be met (e.g. [Kargel et al., 2000](#); [Sephton et al., 2018](#)), with Jupiter's moon Europa receiving particular attention (e.g. [Chyba & Phillips; NASA, 2017](#)).

One hypothesis for life on Europa requires the exchange of oxidants and organics produced on the moon's surface with the subsurface ocean (e.g. [Delitsky & Lane, 1998](#); [Carlson et al., 1999](#); [Chyba, 2000](#); [Chyba & Phillips, 2001](#)), placing an emphasis on 'chaos terrains' as possible locations for major melt-through events of Europa's icy shell ([Carr et al., 1998](#); [Soderlund et al., 2014](#)). However, direct contact between a thin layer of brittle surface ice and an underlying ocean requires an unrealistic amount of thermal energy to locally melt Europa's icy shell ([Collins et al., 2000](#); [Goodman et al., 2004](#)), the thickness of which is poorly constrained but may exceed 30 km ([Sotin et al., 2002](#); [Billings & Kattenhorn, 2005](#); [Fagents et al., 2002](#)). Chaos terrain explanations therefore frequently invoke the presence of a near surface water body emplaced through convective upwelling (e.g. [Sotin et al., 2002](#); [Figueredo et al., 2002](#); [Pappalardo & Carr, 2004](#); [Schmidt et al., 2011](#)) or sills ([Michaut & Manga, 2014](#)) that then reaches the surface through brittle fracturing of the surface (e.g. [Crawford & Stevenson, 1988](#); [Collins et al., 2000](#); [Manga & Wang, 2007](#); [Fagents et al., 2002](#); [Luzzi et al., 2021](#)). Perched water bodies are required in these chaos terrain formation scenarios because the negative buoyancy of water with respect to ice means fractures propagating upwards from the subsurface ocean would extend at most 90% of the way through the shell before reaching hydrostatic equilibrium ([Crawford & Stevenson, 1988](#)).

However, consideration of water bodies perched over ice on Earth strongly suggests that the negative relative buoyancy of water presents a major problem to their stability. Supraglacial lakes, which can exceed 0.125 km² in surface area, pepper the margins of the Greenland Ice Sheet and are readily observed to drain rapidly through hydrofracture ([Das et al., 2008](#); [Doyle et al., 2013](#); [Fitzpatrick et al., 2014](#); [Williamson et al., 2018a](#); [Chudley et al., 2019](#)). Theoretical considerations show that such fractures can penetrate to the ice-sheet bed given a sufficient supply of water, as the density difference

drives fracture propagation ([Weertman, 1973](#); [van der Veen, 2007](#); [Krawczynski et al., 2009](#)). An initial fracture is required for drainage through hydrofracture to occur. This may come from tensile shock from nearby hydrofracture events ([Christoffersen et al., 2018](#)) or a transient strain rate increase (e.g. [Poinar & Andrews, 2021](#)) though it is not clear that there is a single statistically supported explanatory mechanism ([Williamson et al., 2018b](#)). Notably, supraglacial lakes form in surface depressions which are generally dominated by compressive stresses ([Doyle et al., 2013](#); [Stevens et al., 2015](#); [Chudley et al., 2019](#)).

Carnahan et al. ([2022](#)) and Kalousová et al. ([2024](#)) consider the slow downward transport of liquid water through two-phase thermal convection following melt generation from a meteor impact on Europa and Titan respectively, but neglect hydrofracture. In this short paper I suggest that rapid hydrofracture is a plausible downward transport mechanism when a perched water body is present, whether formed through a sill, upwelling convection, or a meteor impact but that a meteor impact provides the most likely scenario due to the accompaniment of ice fracturing and stress perturbation. Such a mechanism may explain chaos terrain formation if violent drainage prompts surface collapse, and provides a clear pathway for the transport of organics and oxidants into the subsurface ocean (Fig. 1). I focus on Europa, but the results are applicable to any ice shell setting.

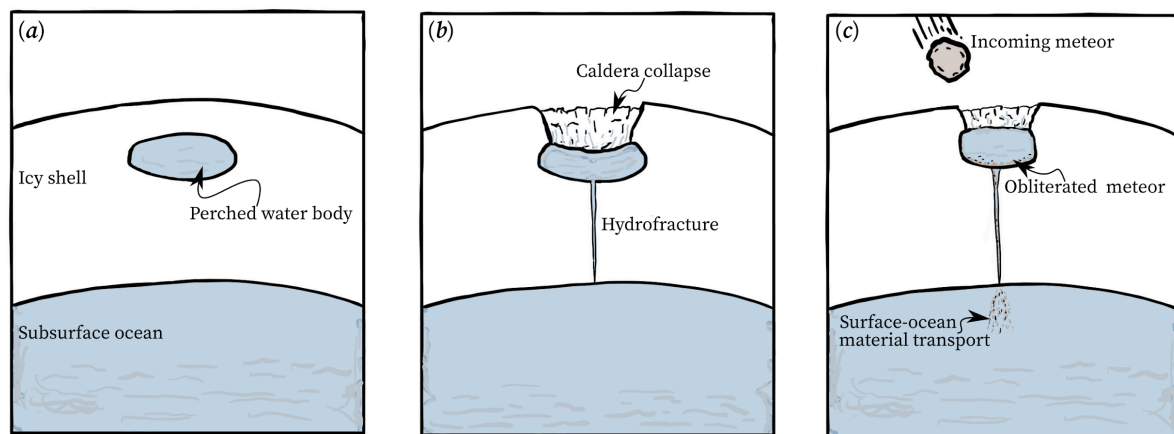


Figure 1: Schematic of icy-shell hydrofracture scenarios covered in the text. (a) A perched water body as hypothesised to form through thermal convection or a sill. **(b)** Hydrofracture resulting in caldera collapse as the perched water body drains. **(c)** Hydrofracture caused by incoming meteor which provides both meltwater and initial fracture and can transport surface material to the subsurface ocean.

Methods

Van der Veen ([1998](#)) calculates terrestrial crevasse propagation under linear elastic fracture mechanics which states that all materials contain small defects which affect the load-bearing capacity of the material. If high stresses concentrate near a defect the defect may propagate and ultimately fracture ([Broek, 1986](#)). In a purely elastic material, an unstable crack will propagate when the energy absorbed by the expansion of a small expansion of the crack is exceeded by the energy released by a small increase in crack size ([Griffith, 1921](#)). This condition is met when the stress intensity factor, K , exceeds the fracture toughness of the material. Ice is not a purely elastic material (instead it has a non-linear viscoelastic rheology), but linear elastic fracture mechanics has proven efficacy in application to terrestrial ice sheets (e.g. [van de Veen, 1998](#); [Chudley et al., 2021](#)). The outer shells of icy moons are likely much colder and therefore much stiffer than terrestrial ice ([Husmann et al., 2002](#)), reducing the importance of the viscous component of rheology ([Goldsby & Kohlstedt, 2001](#)), and melt-formed conduits are a ubiquitous feature of temperate ice alongside fractures ([Fountain & Walder, 1998](#); [Gulley](#)

[et al., 2009](#)). Below I use the essential equations from van der Veen ([1998](#)) and Krawczynski et al. ([2009](#)) and refer the reader to the original papers for more detailed context.

I take a single water filled fracture unaffected by surrounding fractures (Fig. 2) and consider only Mode I fracturing. The stress intensity factor is then determined by three processes which can be superimposed without complication as they all relate to Mode I fracturing. This would not be the case if Mode II and Mode III openings were also considered ([van der Veen, 1998](#)). The far-field tensile stress in Pa^{1/2} given as

$$K^{(1)} = F(\lambda)R_{xx}\pi d \quad (1)$$

where $\lambda = (d + h)/H$, d (m) is the fracture depth, h is the height above the fracture surface to the actual surface, and H is the ice shell thickness (Fig. 2). R_{xx} (Pa) is the resistive stress defined as

$$R_{xx} = \sigma_{xx} - L \quad (2)$$

where σ_{xx} (Pa) is the full stress and $L = \rho_i g(H - z)$ (m) is the lithostatic stress where ρ_i (kg m⁻³) is the density of ice, g (m s⁻²) is acceleration due to gravity and z is 0 at the base of the ice shell increasing upwards. The x and y coordinates are also shown in Fig. 2. The $F(\lambda)$ function is

$$F(\lambda) = 1.12 - 0.23\lambda + 10.55\lambda^2 - 21.72\lambda^3 + 30.39\lambda^4 \quad (3)$$

obtained by polynomial curve fitting to numerically computed stress intensity factors ([Tada et al., 1973](#); [Broek, 1986](#); [van de Veen, 1998](#)).

The net stress intensity factor from the overburden pressure is calculated by integrating the contributions from forces acting at different depths as

$$K^{(2)} = -\frac{2\rho_i g}{\sqrt{\pi d}} \int_0^d bG(\gamma, \lambda)db - \rho_i gh \quad (4)$$

where the $\rho_i gh$ term accounts for the weight of ice overlying the fracture surface. $\gamma = b/d$ and b is the depth from the fracture surface to the point in the fracture under consideration and the function $G(\gamma, \lambda)$ is

$$G(\gamma, \lambda) = \frac{3.52(1-\gamma)}{(1-\lambda)^{3/2}} - \frac{4.35-5.28\gamma}{(1-\lambda)^{1/2}} + \left[\frac{1.30-0.30\gamma^{3/2}}{(1-\gamma^2)^{1/2}} + 0.83 - 1.76\gamma \right] \times [1 - (1 - \gamma)\lambda] \quad (5)$$

again based on numerical curve fitting of numerically derived solutions ([Tada et al., 1973](#); [van de Veen, 1998](#)).

Last, the stress intensity factor from the water pressure within the fracture is

$$K^{(3)} = \frac{2\rho_w g}{\sqrt{\pi d}} \int_a^d (b - a)G(\gamma, \lambda)db \quad (6)$$

where ρ_w is the water density and a is the depth to the water occupying the fracture from the fracture surface. Evaluating the two integrals numerically then gives the net stress intensity factor as

$$K^{(net)} = K^{(1)} + K^{(2)} + K^{(3)} \quad (7)$$

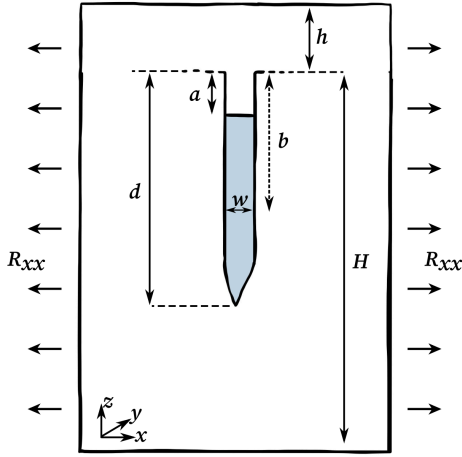


Figure 2: Schematic of fracture calculations. See text for symbol definitions. The dashed line at the top of the fracture is the fracture surface. No perched water body is shown to avoid clutter. In all cases considered in this paper $a = 0$.

The volume of water required for a given crack propagation can then be calculated after Krawczynski et al. (2009) and Weertman (1973). The fracture width, w , at depth b is

$$w(b) = \frac{4\alpha\sigma}{\mu}\omega + \frac{4\alpha\rho_i g d}{\pi\mu}\omega - \frac{4\alpha\rho_w g}{\pi\mu}\omega\psi - \frac{2\alpha\rho_i g b^2}{\pi\mu}\ln\left(\frac{d+\omega}{d-\omega}\right) + \frac{2\alpha\rho_w g(b^2-a^2)}{\pi\mu}\ln\left|\frac{\psi+\omega}{\psi-\omega}\right| - \frac{4\alpha\rho_w g b a}{\pi\mu}\ln\left|\frac{a\omega+b\psi}{a\omega-b\psi}\right| + \frac{4\alpha\rho_w g a^2}{\pi\mu}\ln\left|\frac{\omega+\psi}{\omega-\psi}\right| \quad (8)$$

where μ (Pa) is the shear modulus for ice, $\alpha = (1 - \nu)$ where ν is Poisson's ratio, $\omega = \sqrt{d^2 - b^2}$ and $\psi = \sqrt{d^2 - a^2}$. Here, stress, σ , is expressed as

$$\sigma = R_{xx} - \frac{2\rho_i g H}{\pi} - \rho_w g a + \frac{2\rho_w g a}{\pi}\arcsin\left(\frac{a}{H}\right) + \frac{2\rho_w g}{\pi}\psi. \quad (9)$$

(Contrary to stress calculations for Eqs. 1-7 given the difference in approach between van der Veen 1998 and Krawczynski et al., 2009 which I do not reconcile here.) The fracture volume required for full thickness hydrofracture is given as

$$V = \int_0^H w(b) \quad (10)$$

which is evaluated numerically. I consider a spherical perched water body of radius r , the fracture length l (along the y axis, into the page, and not displayed in Fig. 2) is then taken as $l = \frac{4}{3}r$. On Earth the fracture may at first span the diameter of the water body (Chudley et al., 2019), but a more spherical geometry would result in a shorter fracture length. The radius of the required sphere is

$$r = \sqrt{\frac{V}{\pi}}. \quad (11)$$

The rate of

Values used in calculations are provided in Table 1.

Symbol	Value
g	1.31 m s ⁻²

ν	0.3
ρ_i	917 kg m ⁻³
ρ_w	1000 kg m ⁻³
μ	0.5, 1.5 GPa

Table 1. Values used in calculations.

Results

The calculations demonstrate that under certain circumstances hydrofracture from a perched water body to the subsurface ocean of Europa is possible. Fig. 3 shows the stress intensity fracture that would be experienced at the tip of the fracture against the fracture depth. If the stress intensity at the fracture tip exceeds the critical fracture toughness of ice the fracture will continue to propagate. Given the rate of change of $K^{(3)}$ with depth exceeds that of $K^{(2)}$ for all depths considered, once the stress intensity factor at the fracture tip exceeds the critical fracture toughness the fracture will continue to propagate unbounded, limited only by the water supplying the fracture. An initial fracture depth of only 4.1 m under a tensile stress of 0.1 MPa is required for unstable hydrofracture if the perched water body is located on the surface: such fractures are common across Europa's surface (e.g. [Dombard et al., 2013](#)), but liquid water is not. The critical depth increases significantly as the fracture surface moves further down into the icy shell. Unreasonably deep initial fractures are required in the case of 0 tensile stress (208 m at the surface, 523 m from a fracture surface depth of 1 km).

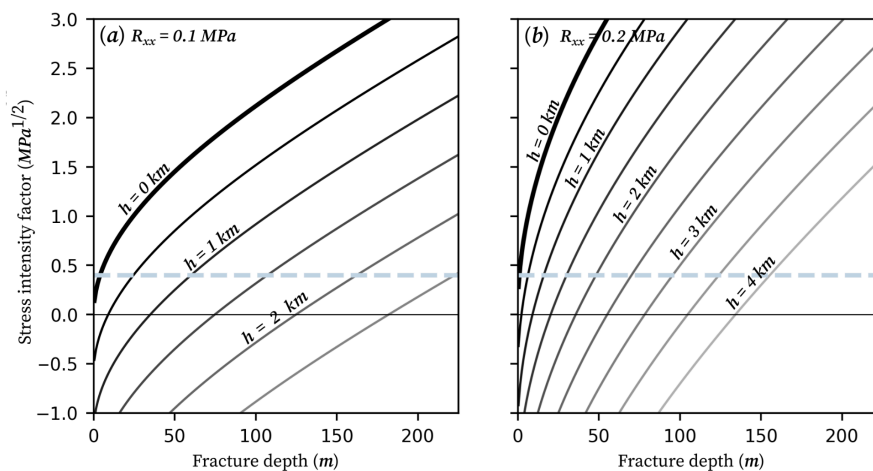


Figure 3: Stress intensity factor as function of fracture depth for varying ice lid thicknesses and tensile stress. The blue dashed line is a reasonable upper limit for the fracture toughness of ice ($0.4 \text{ MPa}^{1/2}$) from van der Veen ([1998](#)). **(a)** Tensile stress is 0.1 MPa. **(b)** Tensile stress is 0.2 MPa.

The volume of water required to facilitate a 30 km fracture under a shear modulus of 1.5 GPa is 38.8 km^3 (Fig. 4), significantly below the $20,000\text{-}60,000 \text{ km}^3$ melt lens estimate of Schmidt et al. ([2011](#)) and an order of magnitude below melt volumes modelled to form by Kalousová et al. ([2024](#)) in the event of moderately sized meteorite impacts. The required water volume is sensitive to the shear modulus and the estimates here follow lower shear modulus values.

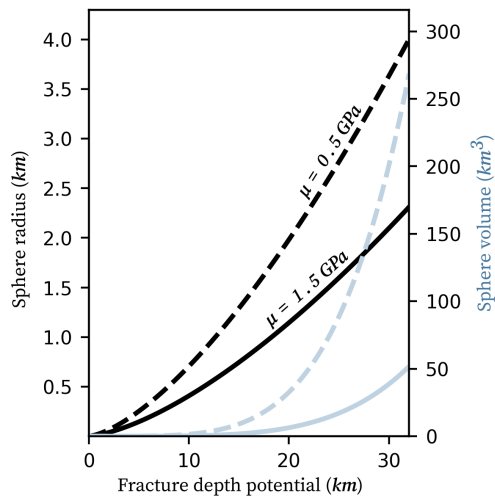


Figure 4: Water volume required for a given fracture depth. Dashed line is for a shear modulus of 0.5 GPa and solid line for 1.5 GPa. Note that the upper bound shear modulus of 3.9 GPa, as used in van der Veen (1998), is not included here. Black indicates required sphere radius, blue indicates shear volume. Assumes a constant width fracture $2/3$ the diameter of the sphere.

Discussion

Figs. 3 and 4 demonstrate that given sufficiently high tensile stresses, initial fracture depth, and latent availability of water, full hydrofracture is possible at Europa. Considering first perched water bodies, this paper demonstrates that tensile stresses much lower than the >20 MPa proposed by Crawford and Stevenson (1988) and Rudolph and Manga (2009) are required for fracture propagation when liquid water is present. Nonetheless, stresses are generally compressive (of order 0.1-0.4 MPa) in Europa's shell (e.g. Pappalardo et al., 1998) meaning hydrofracture of a perched water body would only occur under spatially or temporally limited stress conditions. Structural analysis of surface faults indicate tensile fracturing does occur at the surface of Europa (Kattenhorn & Marshall, 2006) and analysis of the stresses induced by diurnal tides suggests that tensile stresses up to 0.16 MPa are possible (Helfenstein & Parmentier, 1983; Greenberg et al., 1998; Harada & Kurita, 2006; Hurford et al., 2007). While this may allow a fracture of sufficient depth to continue propagating, it cannot immediately account for the formation of the initial crack, particularly in a subsurface setting, though it is worth noting that all mechanisms hypothesised to direct water upwards such as the pressurisation of perched water bodies ought also to work downwards (e.g. Manga & Wang). Crawford and Stevenson (1988) indicate fractures sufficiently deep to initiate hydrofracture may occur under surface stresses of 1-3 MPa, but it is not clear if these tensile stresses are achievable under tidal forcing.

However, while literature on the stress impact of meteor impacts on icy moons is limited, a meteor impact may well provide a tensile shock in excess of 1-3 MPa and a trigger for hydrofracture of perched water bodies, in a similar manner to small but meaningful tensile shocks that can trigger Greenland Ice Sheet lake drainages (Christoffersen et al., 2018). In fact, it is likely that a meteor impacted the Greenland Ice Sheet in its early history with sufficient force to leave a sizeable impact crater beneath the ice (Kjær et al., 2018). It seems unlikely that such an impact would not have led to sizeable fractures forming within the ice. A meteorite impact furthermore likely provides a sufficient water source in the immediate region of the greatest stress disturbance (Kalousová et al., 2024). If incomplete hydrofracture (this paper) or density driven sinking of melt (Carnahan et al., 2022; Kalousová et al., 2024) actually prevent the formation of a perched water body then a meteorite impact becomes the only remaining possible water source.

Van der veen (2007) shows that the key control on the downward propagation of the fracture is the filling rate and that penetration velocity equals the rate of fracture filling to within a few percent. This is because $K^{(2)}$ and $K^{(3)}$ become the dominant terms in Eq. 7 giving

$$d = \left(\frac{\rho_w}{\rho_i} \right)^{\frac{2}{3}} Q t$$

where Q is the vertical fill rate (m s^{-1}) and t (s) is the time period in consideration to a good approximation (Van der veen, 2007). Given a large perched water body positioned over a hydrofracture could therefore be a very rapid phenomena. Supraglacial lakes in Greenland take on the order of 2-3 hours to drain, but the water bodies have an aspect ratio of 1:100 making Q limited by lateral transport from the outer reaches of the lake (Chudley et al., 2019; Das et al., 2008). As a first approximation, even if drainage took 24 hours through ice at 100 K, only 0.34 m of side wall freezing would occur (Appendix A), negligible in the context of a surface opening of 238 m following Eq. 8.

Caldera collapse

Supraglacial lake drainages in Greenland are violent events, capable of throwing up large blocks of ice (Appendix B). If a perched water body within an icy shell drains it not only removes hydrostatic support from the area of ice above it, but it also creates a vacuum that would exert great pressure on the overlying ice roof. If a lake drains in Greenland in winter, a visible fracture pattern is observed at the surface (Russell, 1993), even if the surface ice thickness is only a few metres thick (Law et al., 2020). A similar process but at a far larger scale may well be playing out at Europa and explain the formation of chaos terrains. This supports a more neocatastrophist view of chaos terrain formation than gradual caldera collapse (Luzzi et al., 2021).

Water transport through warm convecting ice

It is challenging to be definitive about the thermal state of Europa's icy shell, but several studies suggest a warm and uniform convecting interior, within around 10 K of the pressure melting point (e.g. McKinnon, 1999; Hussmann et al., 2002; Showman & Han, 2004; Mitri & Showman, 2005). These temperatures are warm relative to an average surface temperature of around 100 K (Ashkenazy, 2019), but their correspondingly lower relative viscosity should not present a problem to elastic fracture given full-thickness hydrofracture through ice of this temperature is common in the Greenland Ice Sheet (e.g. Doyle et al., 2018; Law et al., 2021). More intriguing is the possible influence of temperate ice on water transport within Europa's shell. Carnahan et al. (2022) and Kalousová et al. (2024) do not account for the formation of conduits within the icy shell, yet there are no temperate terrestrial glaciers where there is not some degree of englacial drainage system formation (e.g. Hooke, 1989). A body of temperate ice within an icy shell would lack a supply of surface meltwater, but tidal or convective heating may still produce water internally (e.g. Gaidos & Nimmo, 2000). Given the melt chambers hypothesised by Carnahan et al. (2022) reach >5 km in height and feature melt fractions <5%, it seems reasonable that transport through a drainage system may lead to pooling of water at the transition between temperate and cold ice if fracture does not occur. Further integrating understanding of englacial hydrology with icy moons can advance understanding of these mechanisms.

Conclusions

I have shown that only relatively small tensile stresses, and achievable water volumes, are required for the full hydrofracture of Europa. This has direct application to other icy moons with different gravities and stress regimes, which may also have conditions facilitating full-thickness hydrofracture. It also provides a clear mechanism for the delivery to the subsurface ocean of biologically important materials created on the surface of Europa and delivered by incoming meteorites and may provide an

explanation for the formation of chaos terrains. Hopefully this paper opens further interdisciplinary pathways between glaciology and the study of ice moons.

References

- Alley, R. B., Dupont, T. K., Parizek, B. R., & Anandakrishnan, S. (2005). Access of surface meltwater to beds of sub-freezing glaciers: preliminary insights. *Annals of Glaciology*, 40, 8–14. <https://doi.org/10.3189/172756405781813483>
- Ashkenazy, Y. (2019). The surface temperature of Europa. *Heliyon*, 5(6), 1908. <https://doi.org/10.1016/j.heliyon.2019.e01908>
- Billings, S. E., & Kattenhorn, S. A. (2005). The great thickness debate: Ice shell thickness models for Europa and comparisons with estimates based on flexure at ridges. *Icarus*, 177(2), 397–412. <https://doi.org/10.1016/j.ICARUS.2005.03.013>
- Broek, D. (1982). Elementary engineering fracture mechanics. *Elementary Engineering Fracture Mechanics*. <https://doi.org/10.1007/978-94-009-4333-9>
- Carlson, R. W., Anderson, M. S., Johnson, R. E., Smythe, W. D., Hendrix, A. R., Barth, C. A., Soderblom, L. A., Hansen, G. B., McCord, T. B., Dalton, J. B., Clark, R. N., Shirley, J. H., Ocampo, A. C., & Matson, D. L. (1999). Hydrogen Peroxide on the Surface of Europa. *Science*, 283(5410), 2062–2064. <https://doi.org/10.1126/SCIENCE.283.5410.2062>
- Carnahan, E., Vance, S. D., Cox, R., & Hesse, M. A. (2022). Surface-To-Ocean Exchange by the Sinking of Impact Generated Melt Chambers on Europa. *Geophysical Research Letters*, 49(24), e2022GL100287. <https://doi.org/10.1029/2022GL100287>
- Carr, M. H., Belton, M. J. S., Chapman, C. R., Davies, M. E., Geissler, P., Greenberg, R., McEwen, A. S., Tufts, B. R., Greeley, R., Sullivan, R., Head, J. W., Pappalardo, R. T., Klaasen, K. P., Johnson, T. v., Kaufman, J., Senske, D., Moore, J., Neukum, G., Schubert, G., ... Veverka, J. (1998a). Evidence for a subsurface ocean on Europa. *Nature*, 391(6665), 363–365. <https://doi.org/10.1038/34857>
- Carr, M. H., Belton, M. J. S., Chapman, C. R., Davies, M. E., Geissler, P., Greenberg, R., McEwen, A. S., Tufts, B. R., Greeley, R., Sullivan, R., Head, J. W., Pappalardo, R. T., Klaasen, K. P., Johnson, T. v., Kaufman, J., Senske, D., Moore, J., Neukum, G., Schubert, G., ... Veverka, J. (1998b). Evidence for a subsurface ocean on Europa. *Nature*, 391(6665), 363–365. <https://doi.org/10.1038/34857>
- Cassen, P. M., Peale, S. J., Reynolds, R. T., Ransford, G. A., Finnerty, A. A., Collerson, K. D., Reynolds, R. T.; R. J., Counselman, C. C., King, R. W., Shapiro, I. I., Matson, D. L., Johnson, T. v., Whalley, E., Jones, S. J., Gold, L. W., Eviatar, A., Siscoe, G. L., Lanzcrotti, L. J., Brown, W. L., ... Fanale, F. P. (1983). Liquid water and active resurfacing on Europa. *Nature*, 301(5897), 225–226. <https://doi.org/10.1038/301225a0>
- Christoffersen, P., Bougamont, M., Hubbard, A., Doyle, S. H., Grigsby, S., & Pettersson, R. (2018). Cascading lake drainage on the Greenland Ice Sheet triggered by tensile shock and fracture. *Nature Communications*, 9(1), 1–12. <https://doi.org/10.1038/s41467-018-03420-8>
- Chudley, T. R., Christoffersen, P., Doyle, S. H., Dowling, T. P. F., Law, R., Schoonman, C. M., Bougamont, M., & Hubbard, B. (2021). Controls on Water Storage and Drainage in Crevasses on the Greenland Ice Sheet. *Journal of Geophysical Research: Earth Surface*, 126(9), e2021JF006287. <https://doi.org/10.1029/2021JF006287>
- Chyba, C. F. (2000). Energy for microbial life on Europa. *Nature*, 403(6768), 381–382. <https://doi.org/10.1038/35000281>
- Chyba, C. F., & Phillips, C. B. (2001a). Possible ecosystems and the search for life on Europa. *Proceedings of the National Academy of Sciences of the United States of America*, 98(3), 801–804. <https://doi.org/10.1073/PNAS.98.3.801/ASSET/326781B2-7546-4ECB-9B42-5FB3403EC751/ASSETS/GRAPHIC/PQ0415098001.JPEG>
- Chyba, C. F., & Phillips, C. B. (2001b). Possible ecosystems and the search for life on Europa. *Proceedings of the National Academy of Sciences of the United States of America*, 98(3), 801–804. <https://doi.org/10.1073/PNAS.98.3.801/ASSET/326781B2-7546-4ECB-9B42-5FB3403EC751/ASSETS/GRAPHIC/PQ0415098001.JPEG>
- Collins, G. C., Head, J. W., Pappalardo, R. T., & Spaun, N. A. (2000). Evaluation of models for the formation of chaotic terrain on Europa. *Journal of Geophysical Research: Planets*, 105(E1), 1709–1716. <https://doi.org/10.1029/1999JE001143>
- Crawford, G. D., & Stevenson, D. J. (1988a). Gas-driven water volcanism and the resurfacing of Europa. *Icarus*, 73(1), 66–79. [https://doi.org/10.1016/0019-1035\(88\)90085-1](https://doi.org/10.1016/0019-1035(88)90085-1)
- Delitsky, M. L., & Lane, A. L. (1998). Ice chemistry on the Galilean satellites. *Journal of Geophysical Research: Planets*, 103(E13), 31391–31403. <https://doi.org/10.1029/1998JE900020>
- Dombard, A. J., Patterson, G. W., Lederer, A. P., & Prockter, L. M. (2013). Flanking fractures and the formation of double ridges on Europa. *Icarus*, 223(1), 74–81. <https://doi.org/10.1016/j.ICARUS.2012.11.021>

- Doyle, S. H., Hubbard, A. L., Dow, C. F., Jones, G. A., Fitzpatrick, A., Gusmeroli, A., Kulesa, B., Lindback, K., Pettersson, R., & Box, J. E. (2013a). Ice tectonic deformation during the rapid in situ drainage of a supraglacial lake on the Greenland Ice Sheet. *Cryosphere*, 7(1), 129–140. <https://doi.org/10.5194/TC-7-129-2013>
- Doyle, S. H., Hubbard, A. L., Dow, C. F., Jones, G. A., Fitzpatrick, A., Gusmeroli, A., Kulesa, B., Lindback, K., Pettersson, R., & Box, J. E. (2013b). Ice tectonic deformation during the rapid in situ drainage of a supraglacial lake on the Greenland Ice Sheet. *Cryosphere*, 7(1), 129–140. <https://doi.org/10.5194/TC-7-129-2013>
- Doyle, S. H., Hubbard, B., Christoffersen, P., Young, T. J., Hofstede, C., Bougamont, M., Box, J. E., & Hubbard, A. (2018). Physical Conditions of Fast Glacier Flow: 1. Measurements From Boreholes Drilled to the Bed of Store Glacier, West Greenland. *Journal of Geophysical Research: Earth Surface*, 123(2), 324–348. <https://doi.org/10.1002/2017JF004529>
- Fagents, S. A., Lopes, R. M. C., Quick, L. C., & Gregg, T. K. P. (2022). Cryovolcanism. *Planetary Volcanism across the Solar System*, 161–234. <https://doi.org/10.1016/B978-0-12-813987-5.00005-5>
- Figueredo, P. H., Chuang, F. C., Rathbun, J., Kirk, R. L., & Greeley, R. (2002). Geology and origin of Europa's "Mitten" feature (Murias Chaos). *Journal of Geophysical Research: Planets*, 107(E5), 2–1. <https://doi.org/10.1029/2001JE001591>
- Fitzpatrick, A. A. W., Hubbard, A. L., Box, J. E., Quincey, D. J., van As, D., Mikkelsen, A. P. B., Doyle, S. H., Dow, C. F., Hasholt, B., & Jones, G. A. (2014). A decade (2002–2012) of supraglacial lake volume estimates across Russell Glacier, West Greenland. *Cryosphere*, 8(1), 107–121. <https://doi.org/10.5194/TC-8-107-2014>
- Fountain, A. G., & Walder, J. S. (1998). Water flow through temperate glaciers. *Reviews of Geophysics*, 36(3), 299–328. <https://doi.org/10.1029/97RG03579>
- Gaidos, E. J., & Nimmo, F. (2000). Tectonics and water on Europa. *Nature* 405:6787, 405(6787), 637–637. <https://doi.org/10.1038/35015170>
- Goldsby, D. L., & Kohlstedt, D. L. (2001). Superplastic deformation of ice: Experimental observations. *Journal of Geophysical Research: Solid Earth*, 106(B6), 11017–11030. <https://doi.org/10.1029/2000JB900336>
- Goodman, J. C., Collins, G. C., Marshall, J., & Pierrehumbert, R. T. (2004). Hydrothermal plume dynamics on Europa: Implications for chaos formation. *Journal of Geophysical Research: Planets*, 109(E3), 3008. <https://doi.org/10.1029/2003JE002073>
- Greenberg, R., Geissler, P., Hoppa, G., Tufts, B. R., Durda, D. D., Pappalardo, R., Head, J. W., Greeley, R., Sullivan, R., & Carr, M. H. (1998). Tectonic Processes on Europa: Tidal Stresses, Mechanical Response, and Visible Features. *Icarus*, 135(1), 64–78. <https://doi.org/10.1006/ICAR.1998.5986>
- Griffiths, A. A. (1921). VI. The phenomena of rupture and flow in solids. *Philosophical Transactions of the Royal Society of London. Series A, Containing Papers of a Mathematical or Physical Character*, 4(1), 9–14. <https://doi.org/10.1098/RSTA.1921.0006>
- Gulley, J. D., Benn, D. I., Sreaton, E., & Martin, J. (2009). Mechanisms of englacial conduit formation and their implications for subglacial recharge. *Quaternary Science Reviews*, 28(19–20), 1984–1999. <https://doi.org/10.1016/j.quascirev.2009.04.002>
- Harada, Y., & Kurita, K. (2006). The dependence of surface tidal stress on the internal structure of Europa: The possibility of cracking of the icy shell. *Planetary and Space Science*, 54(2), 170–180. <https://doi.org/10.1016/j.pss.2005.12.001>
- Helpenstein, P., & Parmentier, E. M. (1983). Patterns of fracture and tidal stresses on Europa. *Icarus*, 53(3), 415–430. [https://doi.org/10.1016/0019-1035\(83\)90206-3](https://doi.org/10.1016/0019-1035(83)90206-3)
- Hendrix, A. R., Hurford, T. A., Barge, L. M., Bland, M. T., Bowman, J. S., Brinckerhoff, W., Buratti, B. J., Cable, M. L., Castillo-Rogez, J., Collins, G. C., Diniega, S., German, C. R., Hayes, A. G., Hoehler, T., Hosseini, S., Howett, C. J. A., McEwen, A. S., Neish, C. D., Neveu, M., ... Vance, S. D. (2019). The NASA Roadmap to Ocean Worlds. *Astrobiology*, 19(1), 1–27. <https://doi.org/10.1089/AST.2018.1955/ASSET/IMAGES/LARGE/FIGURE7.JPEG>
- Hurford, T. A., Sarid, A. R., & Greenberg, R. (2007). Cycloidal cracks on Europa: Improved modeling and non-synchronous rotation implications. *Icarus*, 186(1), 218–233. <https://doi.org/10.1016/j.icarus.2006.08.026>
- Husmann, H., Spohn, T., & Wiczerkowski, K. (2002a). Thermal Equilibrium States of Europa's Ice Shell: Implications for Internal Ocean Thickness and Surface Heat Flow. *Icarus*, 156(1), 143–151. <https://doi.org/10.1006/ICAR.2001.6776>
- Kalousová, K., Wakita, S., Sotin, C., Neish, C. D., Soderblom, J. M., Souček, O., & Johnson, B. C. (2024). Evolution of Impact Melt Pools on Titan. *Journal of Geophysical Research: Planets*, 129(3), e2023JE008107. <https://doi.org/10.1029/2023JE008107>

- Kargel, J. S., Kaye, J. Z., Head, J. W., Marion, G. M., Sassen, R., Crowley, J. K., Ballesteros, O. P., Grant, S. A., & Hogenboom, D. L. (2000). Europa's Crust and Ocean: Origin, Composition, and the Prospects for Life. *Icarus*, 148(1), 226–265. <https://doi.org/10.1006/ICAR.2000.6471>
- Kattenhorn, S. A., & Marshall, S. T. (2006). Fault-induced perturbed stress fields and associated tensile and compressive deformation at fault tips in the ice shell of Europa: implications for fault mechanics. *Journal of Structural Geology*, 28(12), 2204–2221. <https://doi.org/10.1016/J.JSG.2005.11.010>
- Khurana, K. K., Kivelson, M. G., Stevenson, D. J., Schubert, G., Russell, C. T., Walker, R. J., & Polansky, C. (1998). Induced magnetic fields as evidence for subsurface oceans in Europa and Callisto. *Nature*, 395(6704), 777–780. <https://doi.org/10.1038/27394>
- Kjær, K. H., Larsen, N. K., Binder, T., Bjørk, A. A., Eisen, O., Fahnestock, M. A., Funder, S., Garde, A. A., Haack, H., Helm, V., Houmark-Nielsen, M., Kjeldsen, K. K., Khan, S. A., Machguth, H., McDonald, I., Morlighem, M., Mouginot, J., Paden, J. D., Waight, T. E., ... MacGregor, J. A. (2018). A large impact crater beneath Hiawatha Glacier in northwest Greenland. *Science Advances*, 4(11). https://doi.org/10.1126/SCIADV.AAR8173/SUPPL_FILE/AAR8173_SM.PDF
- Krawczynski, M. J., Behn, M. D., Das, S. B., & Joughin, I. (2009). Constraints on the lake volume required for hydro-fracture through ice sheets. *Geophysical Research Letters*, 36(10), 10501. <https://doi.org/10.1029/2008GL036765>
- Law, R., Arnold, N., Benedek, C., Tedesco, M., Banwell, A., & Willis, I. (2020). Over-winter persistence of supraglacial lakes on the Greenland Ice Sheet: results and insights from a new model. *Journal of Glaciology*, 66(257), 362–372. <https://doi.org/10.1017/JOG.2020.7>
- Law, R., Christoffersen, P., Hubbard, B., Doyle, S. H., Chudley, T. R., Schoonman, C. M., Bougamont, M., des Tombe, B., Schilperoord, B., Kechavarzi, C., Booth, A., & Young, T. J. (2021). Thermodynamics of a fast-moving Greenlandic outlet glacier revealed by fiber-optic distributed temperature sensing. *Science Advances*, 7(20), 7136–7150. https://doi.org/10.1126/SCIADV.ABE7136/SUPPL_FILE/ABE7136_SM.PDF
- LeB Hooke, R., & LeB Hooke, R. (1989). Arctic and Alpine Research Englacial and Subglacial Hydrology: A Qualitative Review ENGLACIAL AND SUBGLACIAL HYDROLOGY: A QUALITATIVE REVIEW*. *Arctic and Alpine Research*, 21(3), 221–233. <https://doi.org/10.1080/00040851.1989.12002734>
- Lewis, J. S. (1971). Satellites of the outer planets: Their physical and chemical nature. *Icarus*, 15(2), 174–185. [https://doi.org/10.1016/0019-1035\(71\)90072-8](https://doi.org/10.1016/0019-1035(71)90072-8)
- Lorenz, R. D., Stiles, B. W., Kirk, R. L., Allison, M. D., del Marmo, P. P., Iess, L., Lunine, J. I., Ostro, S. J., & Hensley, S. (2008). Titan's rotation reveals an internal ocean and changing zonal winds. *Science*, 319(5870), 1649–1651. https://doi.org/10.1126/SCIENCE.1151639/SUPPL_FILE/LORENZ.SOM.PDF
- Maca Yeal, D. R., Firestone, J., & Adding Ton, E. W. (1993). Supraglacial lake drainage near Sendre Strømmjørd, Greenland. *Journal of Glaciology*, 39(132), 431–433. <https://doi.org/10.3189/S0022143000016105>
- Manga, M., & Wang, C. Y. (2007). Pressurized oceans and the eruption of liquid water on Europa and Enceladus. *Geophysical Research Letters*, 34(7), 7202. <https://doi.org/10.1029/2007GL029297>
- McKinnon, W. B. (1999). Convective instability in Europa's floating ice shell. *Geophysical Research Letters*, 26(7), 951–954. <https://doi.org/10.1029/1999GL900125>
- Michaut, C., & Manga, M. (2014). Domes, pits, and small chaos on Europa produced by water sills. *Journal of Geophysical Research: Planets*, 119(3), 550–573. <https://doi.org/10.1002/2013JE004558>
- Mitri, G., & Showman, A. P. (2005). Convective–conductive transitions and sensitivity of a convecting ice shell to perturbations in heat flux and tidal-heating rate: Implications for Europa. *Icarus*, 177(2), 447–460. <https://doi.org/10.1016/J.ICARUS.2005.03.019>
- NASA. (2017). Europa Lander Study 2016 Report. <https://europa.nasa.gov/resources/58/europa-lander-study-2016-report/>
- Pappalardo, R. T., & Barr, A. C. (2004). The origin of domes on Europa: The role of thermally induced compositional diapirism. *Geophysical Research Letters*, 31(1). <https://doi.org/10.1029/2003GL019202>
- Pappalardo, R. T., Head, J. W., Greeley, R., Sullivan, R. J., Pilcher, C., Schubert, G., Moore, W. B., Carr, M. H., Moore, J. M., Belton, M. J. S., & Goldsby, D. L. (1998). Geological evidence for solid-state convection in Europa's ice shell. *Nature* 1998 391:6665, 391(6665), 365–368. <https://doi.org/10.1038/34862>
- Poinar, K., & C. Andrews, L. (2021). Challenges in predicting Greenland supraglacial lake drainages at the regional scale. *Cryosphere*, 15(3), 1455–1483. <https://doi.org/10.5194/TC-15-1455-2021>

Porco, C. C., Helfenstein, P., Thomas, P. C., Ingersoll, A. P., Wisdom, J., West, R., Neukum, G., Denk, T., Wagner, R., Roatsch, T., Kieffer, S., Turtle, E., McEwen, A., Johnson, T. v., Rathbun, J., Veverka, J., Wilson, D., Perry, J., Spitale, J., ... Squyres, S. (2006). Cassini observes the active south pole of Enceladus. *Science*, 311(5766), 1393–1401. https://doi.org/10.1126/SCIENCE.1123013/SUPPL_FILE/PORCOCC.SOM.PDF

Rubin, A. M. (2003). Propagation of Magma-Filled Cracks. <https://doi.org/10.1146/annurev.Ea.23.050195.001443>, 23, 287–336. <https://doi.org/10.1146/annurev.Ea.23.050195.001443>

Rudolph, M. L., & Manga, M. (2009). Fracture penetration in planetary ice shells. *Icarus*, 199(2), 536–541. <https://doi.org/10.1016/j.icarus.2008.10.010>

Schmidt, B. E., Blankenship, D. D., Patterson, G. W., & Schenk, P. M. (2011). Active formation of ‘chaos terrain’ over shallow subsurface water on Europa. *Nature*, 479(7374), 502–505. <https://doi.org/10.1038/nature10608>

Sephton, M. A., Waite, J. H., & Brockwell, T. G. (2018). How to detect life on icy moons. *Astrobiology*, 18(7), 843–855. <https://doi.org/10.1089/ast.2017.1656/asset/images/large/figure5.jpeg>

Showman, A. P., & Han, L. (2004). Numerical simulations of convection in Europa’s ice shell: Implications for surface features. *Journal of Geophysical Research: Planets*, 109(E1), 1010. <https://doi.org/10.1029/2003JE002103>

Soderlund, K. M., Schmidt, B. E., Wicht, J., & Blankenship, D. D. (2013). Ocean-driven heating of Europa’s icy shell at low latitudes. *Nature Geoscience*, 7(1), 16–19. <https://doi.org/10.1038/ngeo2021>

Sotin, C., Head, J. W., & Tobie, G. (2002). Europa: Tidal heating of upwelling thermal plumes and the origin of lenticulae and chaos melting. *Geophysical Research Letters*, 29(8), 74–1. <https://doi.org/10.1029/2001GL013844>

Tada, H., Paris, P. C., & Irwin, G. (1973). *The Stress Analysis of Cracks Handbook*.

van der Veen, C. J. (1998). Fracture mechanics approach to penetration of bottom crevasses on glaciers. *Cold Regions Science and Technology*, 27(3), 213–223. [https://doi.org/10.1016/S0165-232X\(98\)00006-8](https://doi.org/10.1016/S0165-232X(98)00006-8)

van der Veen, C. J. (2007). Fracture propagation as means of rapidly transferring surface meltwater to the base of glaciers. *Geophysical Research Letters*, 34(1). <https://doi.org/10.1029/2006GL028385>

Weertman, J. (1973). Can a water-filled crevasse reach the bottom surface of a glacier. *Symposium of the Hydrology of Glaciers*, 139–145.

Williamson, A. G., Banwell, A. F., Willis, I. C., & Arnold, N. S. (2018). Dual-satellite (Sentinel-2 and Landsat 8) remote sensing of supraglacial lakes in Greenland. *Cryosphere*, 12(9), 3045–3065. <https://doi.org/10.5194/TC-12-3045-2018>

Williamson, A. G., Willis, I. C., Arnold, N. S., & Banwell, A. F. (2018). Controls on rapid supraglacial lake drainage in West Greenland: an Exploratory Data Analysis approach. *Journal of Glaciology*, 64(244), 208–226. <https://doi.org/10.1017/JOG.2018.8>

Acknowledgments

Thanks to Craig Walton and Claire Guimond for introducing me to this field. I acknowledge funding from Norges forskningsråd.

Appendix A

Freeze onto a side wall, W (m) calculated as

$$W(t) = \frac{2C(T_m - T_o)}{\sqrt{\pi L}} \sqrt{kt}$$

where $C = 2093 \text{ J kg}^{-1} \text{ K}^{-1}$ is the specific heat, $k = 1.18 \times 10^{-6} \text{ m}^2 \text{ s}^{-1}$ is the thermal diffusivity, $L = 3.3 \times 10^5 \text{ J kg}^{-1}$ is the latent heat of ice, T_m is the melting point of ice, and T_o is the temperature of the ice wall ([Rubin, 1995](#); [Alley et al., 2005](#)).

Appendix B



Appendix A: The immediate aftermath of a supraglacial lake drainage. Photo credit: Poul Christoffersen.